

4. NOISE FIGURE SUMMARIES

In this section we present distribution functions of median, mean, and peak noise powers, we describe and compare the measurement and analysis methods to those used by the CCIR, and we conclude by contrasting the noise figure results with those used by the CCIR.

4.1 Distribution Functions of Median, Mean, and Peak Powers

We began our noise figure analysis by constructing distribution functions of median, mean, and peak powers for rural, residential, and business environments. These values were derived from measurement histograms spaced approximately one hour apart. The distribution functions were plotted on a normal probability graph where a Gaussian distributed variable is represented by a straight line whose mean lies on the 50th percentile and slope is the standard deviation. The distribution functions shows the probability that the median, mean, or peak exceeds a particular value.

The mean, in these plots, is the antenna noise figure, F_a , derived from

$$F_a = 10\log_{10}(f - f_r + 1) \quad (4.1)$$

where, recalling the notation in Section 1, f is the measured noise factor and f_r is the receiver noise factor. In a similar way the median value is

$$G_a = 10\log_{10}(g - g_r + 1) . \quad (4.2)$$

In this case g represents the measured median noise power and g_r represents the receiver median noise power. This correction is based on the somewhat dubious approximation [13] that the median of a convolution is the sum (or difference) of the two component medians. The peak value is uncorrected and represents the measured noise power in dB above kT_0b that is exceeded 0.01 percent of the time.

Figure 4.1 shows the distribution function of G_a , F_a , and peak power over a 4-day period at the Lakewood, Colorado, residential site described in Section 3. In Figure 4.2 we have plotted the F_a for both residential sites. Note how the median F_a varies for the two locations. Figure 4.3 shows the G_a , F_a , and peak power for the two residences combined.

Similarly in Figure 4.4 the distribution functions for the F_a of six business locations are displayed. There seems to be two populations - a noisy, "business" set and a quieter, "light urban" set. The center of the office park falls within the business set, while locations adjacent to interstate highways fall within the light urban set. Figures 4.5 and 4.6 show the G_a , F_a , and peak power for each population. Only measurements taken during working hours were used.

Figure 4.7 shows the combined data from four rural locations. All of the measurements included in the distribution were taken during working hours. Cummulative distribution functions for each rural

location are not shown because of the short measurement periods involved. While the peak is considerably less than that observed in other environments, it still exceeds Gaussian noise values. Thus, even in rural areas, there is impulsive noise.

4.2 Comparison of Measurement and Modeling Methods

4.2.1 Measurement and Analysis Methods used by CCIR

CCIR methods for predicting man-made noise factors are based on approximately 300 hours of noise measurements at 31 rural-, 38 residential-, and 23 business-environment “measurement areas” [1]. The measurements were obtained during “mobile runs” through the measurement area, which ranged in size from a few city blocks for a business environment to several square kilometers for a rural environment. The mobile run was typically made during working hours and lasted approximately one hour. Eight frequencies ranging from 250 kHz to 250 MHz were measured simultaneously.

The objective was to estimate each environment F_{am} defined as the average noise power that can be expected in 50% of the measurement areas for 50% of the time within-the-hour. To accomplish this objective the mobile runs were sorted according to environment, and the median F_a of each mobile run was determined. Since the mobile runs lasted approximately one hour this median represented the hourly median F_a . The hourly median F_a values were plotted as a function of frequency, and a linear regression line representing the environment F_{am} across the frequency range was determined. A similar procedure was used to determine the environment within-the-hour upper and lower deciles of F_a represented by D_u and D_l , respectively.

The standard deviation of the hourly median F_a values from the environment F_{am} value is defined as the *location variability*, F_L . The D_u and D_l can be combined to represent the *within-the-hour time variability*

$$\sigma_T = \frac{1}{1.28} \left[\frac{D_u^2 + D_l^2}{2} \right]^{\frac{1}{2}} . \quad (4.3)$$

Finally the *composite variability* represents the location- and within-the-hour time- variability

$$\sigma_c = \sqrt{\sigma_L^2 + \sigma_T^2} . \quad (4.4)$$

Using these parameters, the behavior of F_a can be modeled by

$$F_a = F_{am} + y_L(l) + y_T(t) . \quad (4.5)$$

where y_L and y_T represent location and time deviations, which are zero-mean Gaussian distributions with standard deviations of F_L and F_T , respectively.

4.2.2 Measurement and Analysis Method Used by this Study

We analyzed approximately 100 hours of noise measurements in 4 rural-, 2 residential-, and 6 business-environment locations. Our measurements were obtained while the measurement van was parked and only noise at a single frequency was measured. Rural measurement durations were typically less than an hour, residential measurement durations were often more than 24 hours, and business measurement durations varied from 1 to more than 24 hours.

Our measurements indicated that F_a changed little within the hour. This is in contrast to the 6.6 dB F_T , independent of environment or frequency, reported by Spaulding and Stewart [14]. One consequence of a negligible F_T is that it was not necessary to determine the hourly median F_a of a location. Instead, sampling F_a once per hour (avoiding satellite passes) is sufficient for any location. The distributions of the sampled F_a are shown in Figures 4.3, 4.5, 4.6, and 4.7. The median of the sampled F_a represents the median over all hours and locations measured. This median can be compared to the F_{am} used by the CCIR methods. The standard deviation of the sampled F_a can be compared to CCIR method F_L since F_T was negligible.

4.3 Noise Figure Predictions.

Table 1 shows our measured F_{am} and F compared to values in CCIR Recommendations. Business and rural environment F_{am} fall within one standard deviation of CCIR Recommendations; however, residential F_{am} has decreased dramatically and is more than two standard deviations from CCIR Recommendations. This indicates that residential noise power may have decreased.

Table 1. Measured Noise Figure Statistics Compared to CCIR Recommendations at 137 MHz

Environment	Measured		CCIR Recommendations	
	F_{am} (dB)	F (dB)	F_{am} (dB)	F_L (dB)
Business	18.0	2.6	17.6	8.0
Light Urban	8.5	5.8	----	----
Residential	6.0	2.9	13.3	2.7
Rural	6.3	1.5	8.0	3.2

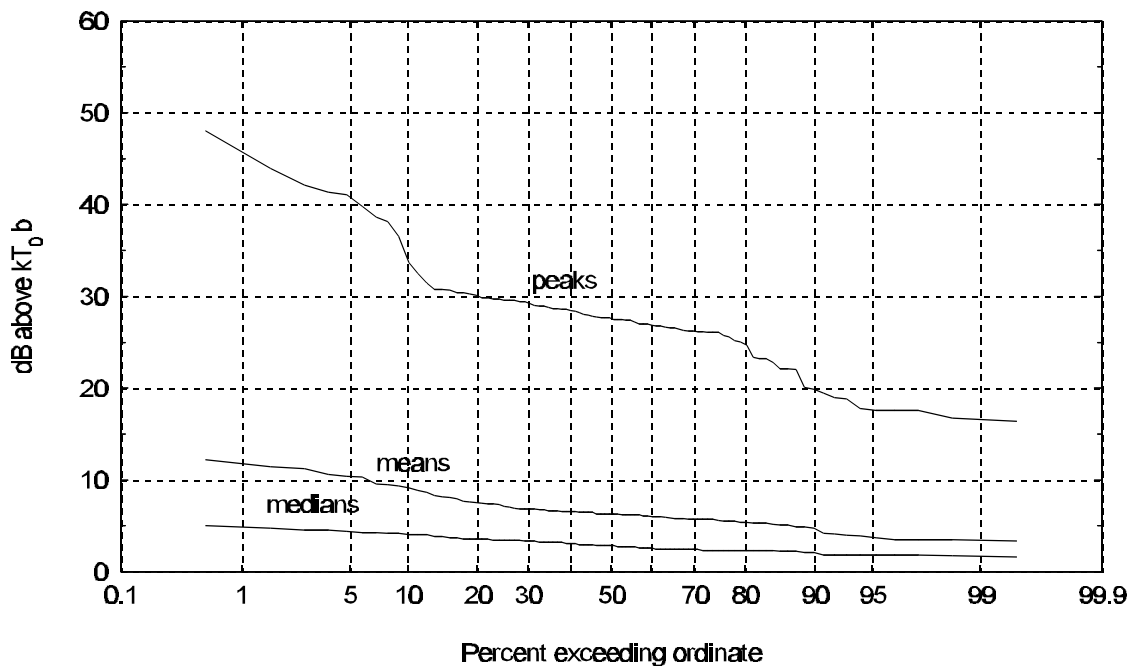


Figure 4.1 Cumulative distribution functions of the median, mean, and peak values for a 4-day sequence of measurements at the Lakewood, Colorado, residential location.

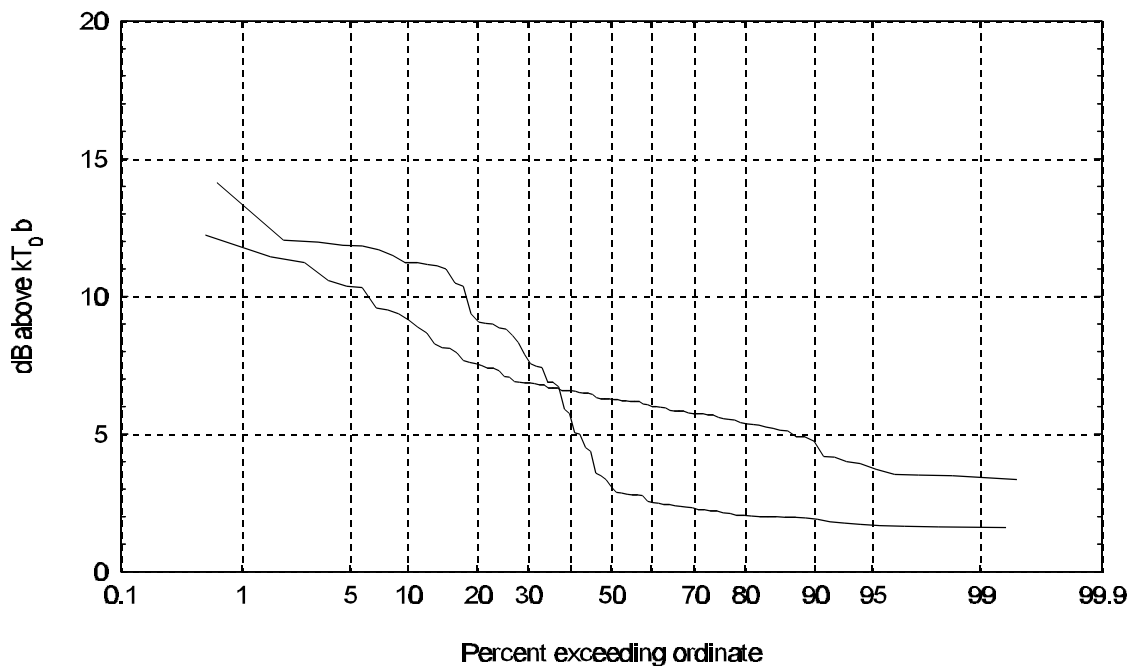


Figure 4.2 Cumulative distribution functions of the mean values for two residential locations.

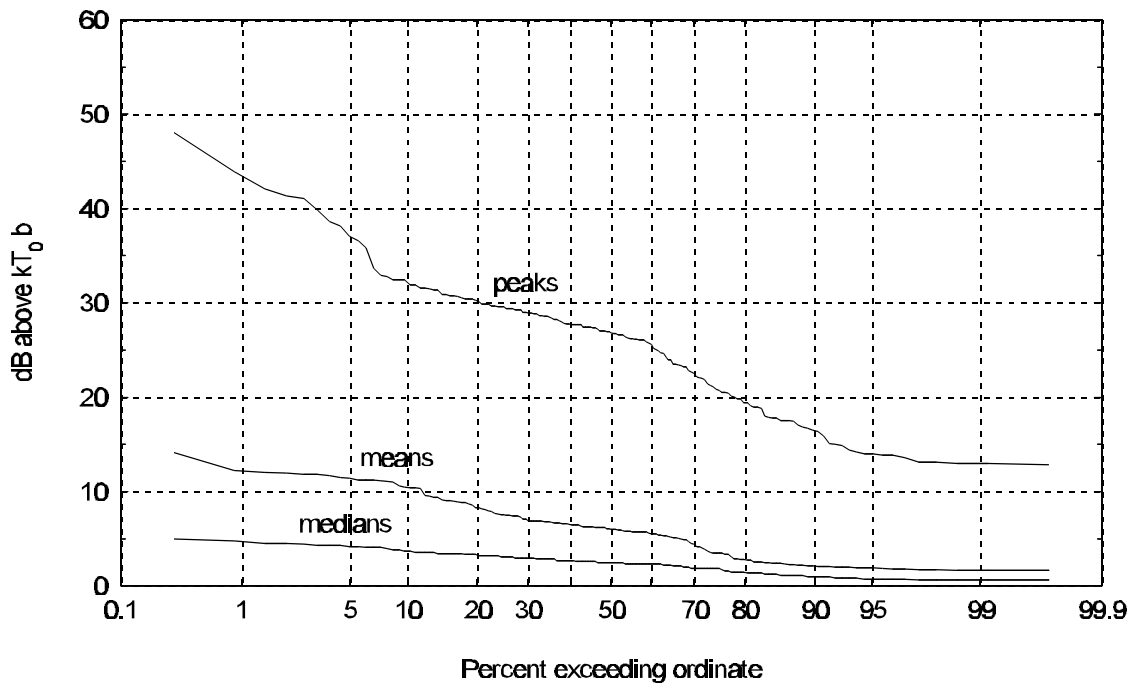


Figure 4.3 Cumulative distribution functions of the combined median, mean, and peak values of Lakewood, Colorado, and Boulder, Colorado, residential locations.

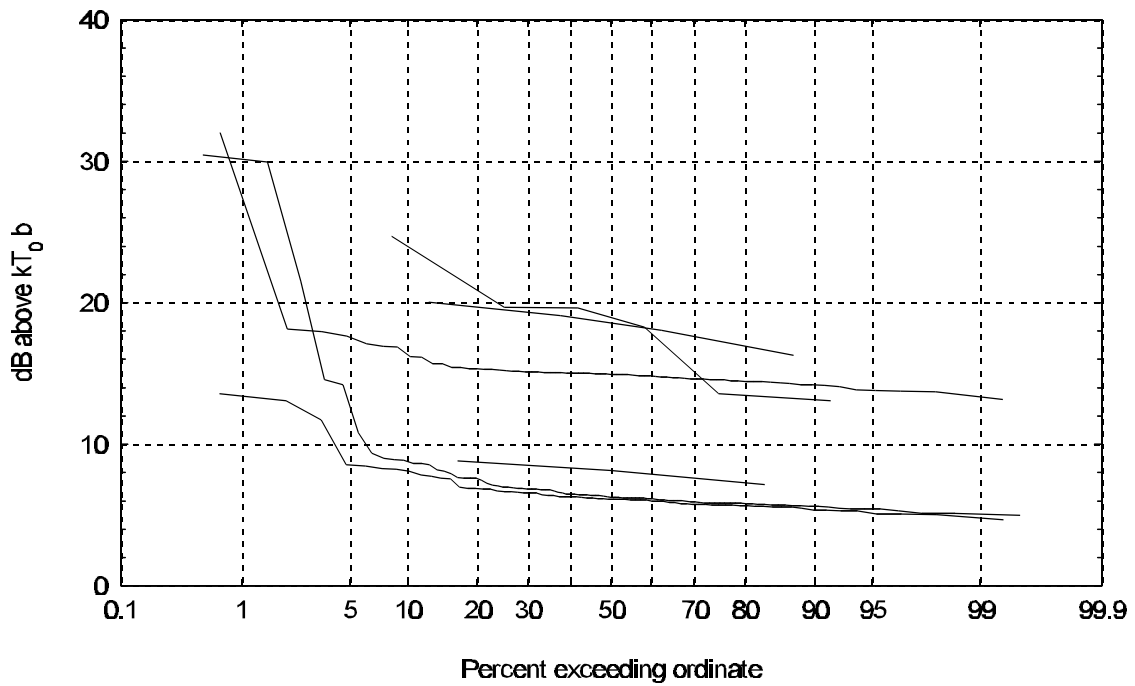


Figure 4.4 Cumulative distribution functions of the mean values for six business locations.

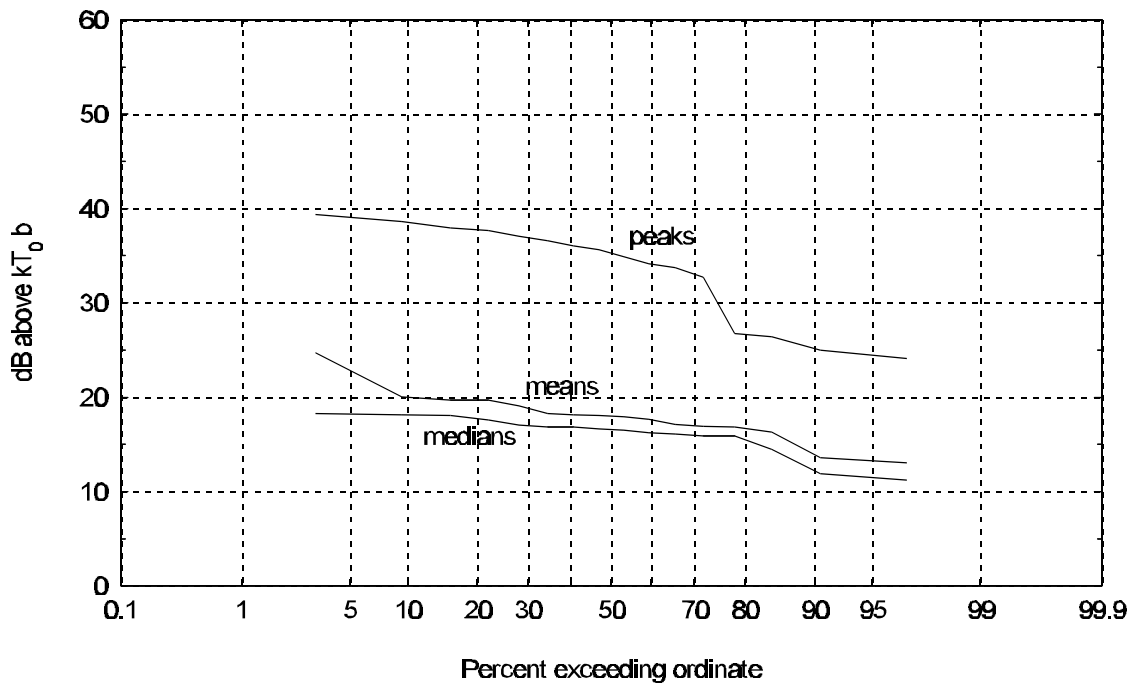


Figure 4.5 Cumulative distribution functions of combined median, mean, and peak values for three business locations.

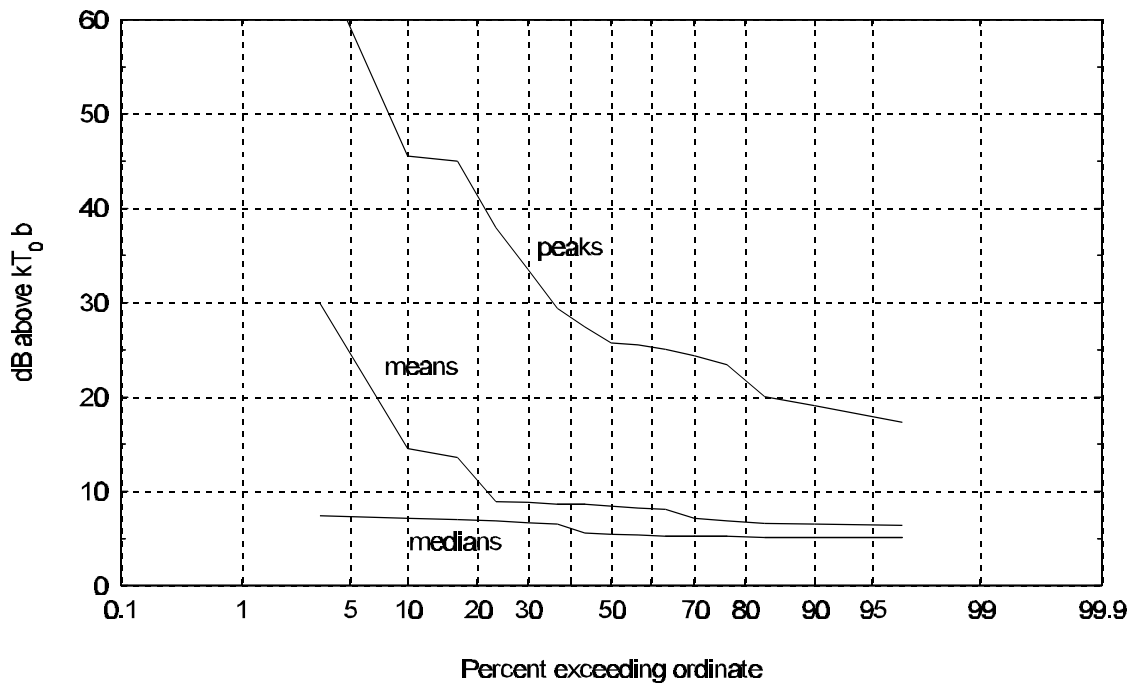


Figure 4.6 Cumulative distribution functions of combined median, mean, and peak values for three "light urban" locations.

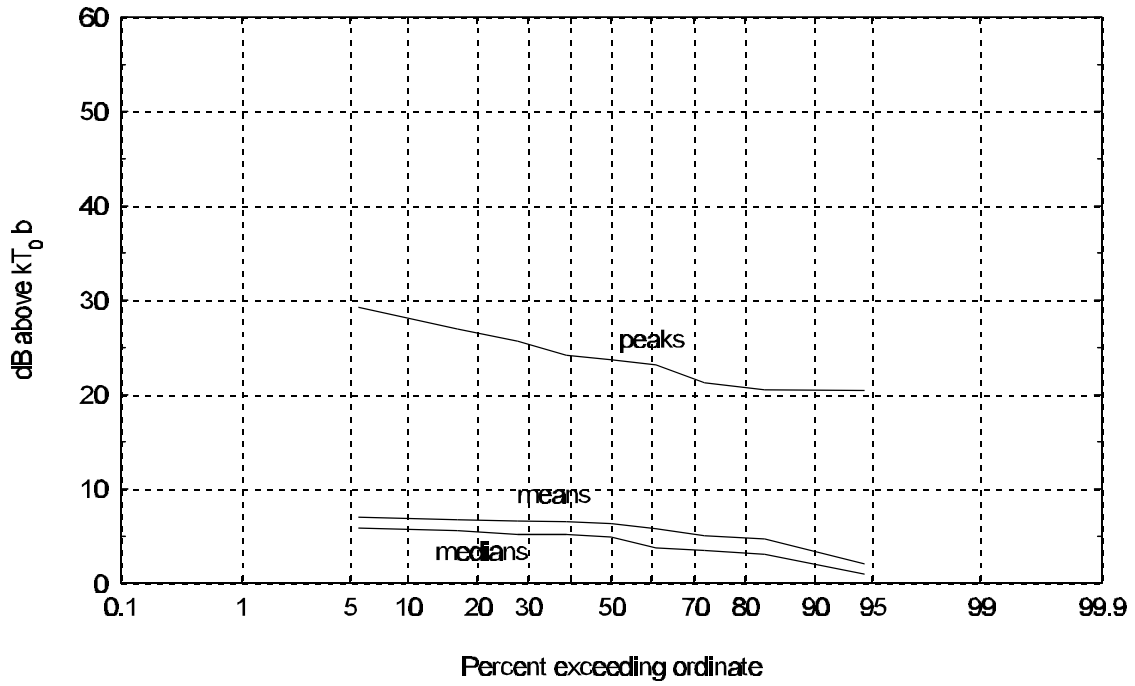


Figure 4.7 Cumulative distribution functions of combined median, mean, and peak values for four rural locations.